RNA (1997), 3:489-497. Cambridge University Press. Printed in the USA.

Importance of structural features for tRNA^{Met} identity

RUSLAN APHASIZHEV,* BRUNO SENGER,* and FRANCO FASIOLO

CNRS, UPR 9002 Structure des Macromolécules Biologiques et Mécanismes de Reconnaissance, Institut de Biologie Moléculaire et Cellulaire, 15 Rue René Descartes, F-67084 Strasbourg, France

ABSTRACT

We showed previously that the tRNA tertiary structure makes an important contribution to the identity of yeast tRNA^{Met} (Senger B, Aphasizhev R, Walter P, Fasiolo F, 1995, *J Mol Biol 249*:45–58). To learn more about the role played by the tRNA framework, we analyzed the effect of some phosphodiester cleavages and 2′OH groups in tRNA binding and aminoacylation. The tRNA is inactivated provided the break occurs in the central core region responsible for the tertiary fold or in the anticodon stem/loop region. We also show that, for tRNA^{Met} to bind, the anticodon loop, but not the anticodon stem, requires a ribosephosphate backbone. A tertiary mutant of yeast tRNA^{Met} involving interactions from the D- and T-loop unique to the initiator species fails to be aminoacylated, but still binds to yeast methionyl-tRNA synthetase. In the presence of 10 mM $MgCl_2$, the mutant transcript has a 3D fold significantly stabilized by about 30 °C over a wild-type transcript as deduced from the measure of their T_m values. The k_{cat} defect of the tRNA^{Met} mutant may arise from a failure to overcome an increase of the free energetic cost of distorting the more stable tRNA structure and/or a tRNA based MetRS conformational change required for formation of transition state of aminoacylation.

Keywords: DNA–RNA anticodon minihelix; melting profiles; methionine tRNA; phosphodiester cleavage; tertiary structure

INTRODUCTION

The highly selective recognition of any DNA or RNA site by a protein most commonly relies on a network of hydrogen bonds with specific bases Draper (1995). In the case of tRNAs, base-specific contacts with the cognate synthetase were deduced from the effect base substitutions on the kinetic parameter k_{cat}/K_m of tRNA aminoacylation and from tRNA identity swap experiments. These contacts are generally in the anticodon and/or at the last base pairs of the acceptor stem, including the discriminatory base at position 73 (for recent reviews see: Giégé et al., 1993; McClain, 1993; Saks et al., 1994). The existence of direct protein-base contacts suggested by the genetic experiments was further confirmed by the crystal structure of tRNA-synthetase complexes involving either *Escherichia coli* glutaminyl- (Rould et al., 1989) or yeast aspartyl-tRNA synthetase (Ruff et al., 1991). These co-complexes also revealed the existence of numerous protein-phosphate backbone contacts, which probably contribute indirectly to the tRNA binding specificity. The large excess of binding energy provided by these contacts may be used to deform the tRNA in the anticodon (Rould et al., 1991; Ruff et al., 1991) and the acceptor end (Rould et al., 1989). In the case of the tRNA^{Gln}-GlnRS complex, distortion of the CCA-end into a hairpin structure is an important thermodynamic feature for binding and catalysis. Deformability of the nucleic acid structure is a common theme in RNA and DNA recognition (Draper, 1993, 1995), and a careful thermodynamic study revealed that sequence discrimination of the DNA site by *Eco*R I-endonuclease is strongly dependent on the energetic cost of distorting the DNA to achieve optimal DNA-protein complementarity (Lesser et al., 1990, 1993).

In a previous work, we identified the primary (Senger et al., 1992), secondary, and tertiary determinants (Senger et al., 1995) required for efficient aminoacylation of tRNA^{Met} by yeast methionyl-tRNA synthetase (MetRS). The demonstration that the tRNA tertiary structure is part of tRNA^{Met} identity suggests the contribution of a number of protein-phosphate backbone contacts in the specificity of tRNA binding. Analysis of the *Thermus thermophilus* tRNA^{Ser}-seryl-tRNA synthetase crystal structure has shown clearly that extensive protein contacts with the backbone of the variable arm

Reprint requests to: Franco Fasiolo, IBMC, 15 Rue Descartes, F-67084 Strasbourg, France.

*Both authors contributed equally to the work.

contribute predominantly to the specificity of $tRNA^{Ser}$ recognition (Biou et al., 1994). In the absence of a co-crystal structure, protein-ribose contacts could be deduced from biochemical studies using mixed DNA-RNA hybrid minihelices or 3/4 tRNA molecules. In this way, three 2'OH groups within 5 Å of the unpaired exocyclic amine of G3 were found to contribute to the recognition and aminoacylation of $tRNA^{Ala}$ (Musier-Forsyth & Schimmel, 1992) and, in the case of $tRNA^{Pro}$, a ribose 2'OH group contact within the core region of the tRNA is important for aminoacylation (Yap & Musier-Forsyth, 1995).

The aim of this study was to analyze a number of contributions other than specific bases to $tRNA^{Met}$ aminoacylation. We checked the effect of a limited number of single phosphate backbone breaks scattered within the tRNA molecule as well as the role of 2'OH ribose groups in the binding of mixed RNA-DNA anticodon hairpin variants. Finally, by using, for the first time, a temperature-gradient gel electrophoresis (TGGE)-based method to understand the deleterious effect of a tertiary mutant (Senger et al., 1995), we could show that the lack of aminoacylation correlates with an increased stability of mutant the tRNA as compared to the wild-type tRNA. This result was confirmed by the measure of the T_m values in presence and absence of $MgCl_2$.

RESULTS

Synthesis and activity of nicked $tRNA^{Met}$ molecules

Studies with minihelices that recreate the TΨC-acceptor and anticodon arm of $tRNA^{Met}$ already established the need for a covalent continuity between the anticodon and the acceptor end for the activity of the tRNA (Senger et al., 1995). In this analysis, the function of the two tRNA domains was tested independently from the tRNA tertiary structure so that the role of a particular backbone bond on tRNA folding and activity could not be addressed. A method, termed circular permutation analysis (CPA), was developed in which the effect of a single break on tRNA folding can be analyzed in a single experiment provided that the 5' and 3' ends of the RNA molecule are first joined covalently (Pan et al., 1991). This method was extended to the study of RNA-protein (Gott et al., 1993; Pan & Uhlenbeck, 1993) or RNA-RNA binding sites (Pan & Zhong, 1994) and reveals that many of the phosphodiester bonds in the RNA can be broken with little or no effect on RNA folding or activity unless the breaks occur in highly conserved regions of the RNA or in the protein (or RNA) binding site.

We introduced selected breaks in $tRNA^{Met}$ at position 8, 28, 34, and 53, by annealing the corresponding complementary tRNA fragments generated by T7 RNA transcription (Fig. 1) and tested the effect on tRNA aminoacylation. Mixing two halves or 3/4 and 1/4 molecules is compatible with tertiary structure formation as shown in previous studies by measuring the aminoacylation activity and magnitude of the enthalpy change (Coutts et al., 1974) or the electrophoretic mobility of the nicked tRNA (Liu & Musier-Forsyth, 1994). In the case of $tRNA^{Met}$, each of the nicked molecules was resolved in a major band that comigrated with wild-type $tRNA^{Met}$ on a native polyacrylamide gel, except hybrid (1-52, 53-76), where only 25% of the RNA migrated as a tRNA band (results not shown). This hybrid is the only active nicked $tRNA^{Met}$ (Fig. 2). Its catalytic efficiency of aminoacylation is about 0.08 that of wild-type $tRNA^{Met}$ transcript after correction for the yield of nicked tRNA and for the concentration of enzyme used. This activity can be explained by the fact that the energy of RNA folding in helical stem-loop regions (here the TΨC stem) is sufficiently high to compensate for a single phosphodiester bond cleavage (Pan & Uhlenbeck, 1993), thus allowing tertiary structure formation. Inactivation resulting from a cut at position 8 was predicted by the model of Pan and Uhlenbeck (1993) because the phosphodiester break probably disrupts the sharp bend between G9 and G10 and affects the highly ordered structure of the central core region. The importance of $tRNA^{Met}$ anticodon loop in tRNA binding and activity (Despons et al., 1992; Senger et al., 1995) may explain the deleterious effect of a phosphodiester break at position 34 because the integrity of the major tRNA binding site is probably disrupted by this cut. Inactivation by a cut in the anticodon stem (position 28) is rather surprising, because this position is not part of the contact area between the $tRNA^{Met}$ and MetRS (Perona et al., 1991); however, this result is in line with other studies, which showed a change in the structure and activity of the anticodon loop through the influence of the adjacent stem (Yarus et al., 1986; Seong & RajBhandary, 1987).

Binding of mixed RNA–DNA $tRNA^{Met}$ anticodon minihelices to yeast MetRS

We showed previously that a $tRNA^{Met}$ anticodon minihelix contains the major determinants for MetRS binding based on the K_i value of competitive inhibition in the aminoacylation reaction (Senger et al., 1995). A DNA version of the anticodon minihelix failed, however, to bind yeast MetRS. To identify the structural requirements important for MetRS-anticodon interaction, we tested the inhibition of $tRNA^{Met}$ aminoacylation provided by mixed ribodeoxy-anticodon minihelices. In the first version, a tDNA stem is associated with a ribo-anticodon loop, whereas in the second, a deoxy-anticodon loop is associated with an RNA anticodon stem (Fig. 3A). These variants were obtained by chemical RNA-DNA synthesis. The results of the inhibition

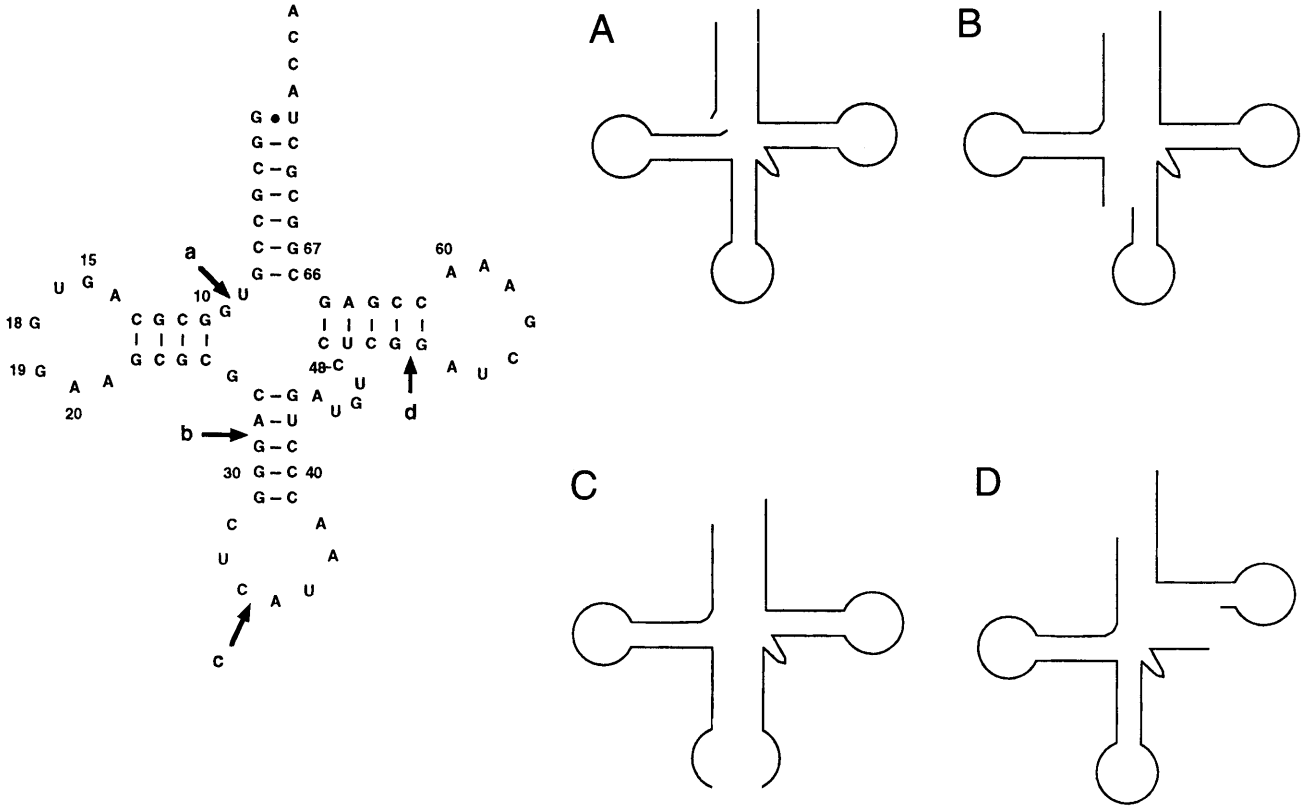

FIGURE 1. Cloverleaf structure of yeast initiator tRNA^{Met} and derived nicked variants. Dot on the cloverleaf structure indicates that wild-type A1U72 base pair was replaced by G1U72 to improve the efficiency of T7 RNA transcription (Senger et al., 1992). Arrows indicate the various single cuts introduced in the tRNA^{Met} sequence and the resulting 5′ and 3′ fragments are represented on a schematic drawing of the tRNA^{Met} molecule. Various hybrids obtained by annealing fragments as follows. **A:** 1-9 and 10-76. **B:** 1-28 and 29-76. **C:** 1-34 and 35-76. **D:** 1-52 and 53-76.

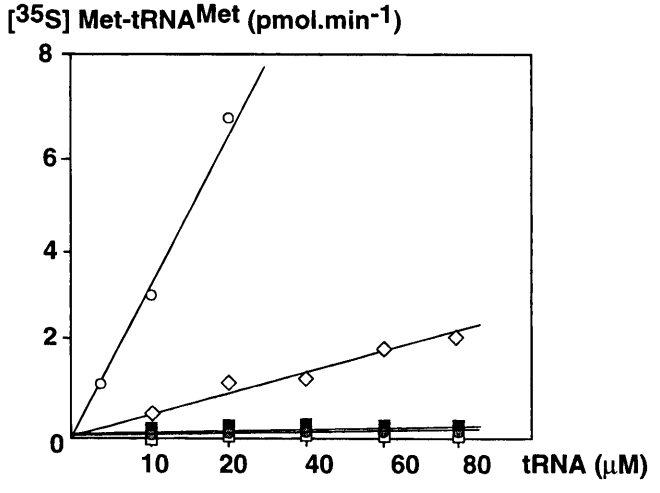

FIGURE 2. Aminoacylation of the nicked tRNA^{Met} molecules. After annealing of the complementary tRNA^{Met} fragments, an aliquot of the mixture was analyzed on a 10% native polyacrylamide gel and the renaturation of the nicked was assessed by comigration with wild-type tRNA^{Met} transcript (see Materials and Methods). The concentration of MetRS in the test was 10 nM for wild-type tRNA^{Met} transcript, 500 nM for hybrids (**A**), (**B**), and (**C**), and 100 nM for hybrid (**D**).

studies show that only the first variant is a powerful inhibitor (Fig. 3B). The double reciprocal plot of initial velocities versus substrate concentration at varied concentrations of inhibitor favor a model of competitive inhibition (Fig. 3C), but not of uncompetitive inhibition. These results indicate that, for the anticodon hairpin to bind, RNA sequences from the anticodon loop cannot be replaced by corresponding DNA sequences, whereas that of the anticodon stem can. Clues explaining this result may come from recent work of Basti et al. (1996), who compared the anticodon structure of the yeast tRNA^{Phe} crystal with that of a DNA analogue in solution. The NMR studies revealed that the stem helical width of the anticodon DNA variant (19.7 Å) is more related to that of the tRNA anticodon domain (20.4 Å) than to the 26 Å width of A-RNA. They also found that the distances between base-centered pseudoatoms of the tDNA and tRNA stem regions are similar. In contrast, distances from bases of the stem to those of the loops and the angle between stem and loop are different. These structural divergences still allow ribosome binding (Basti et al., 1996), but they can nega-

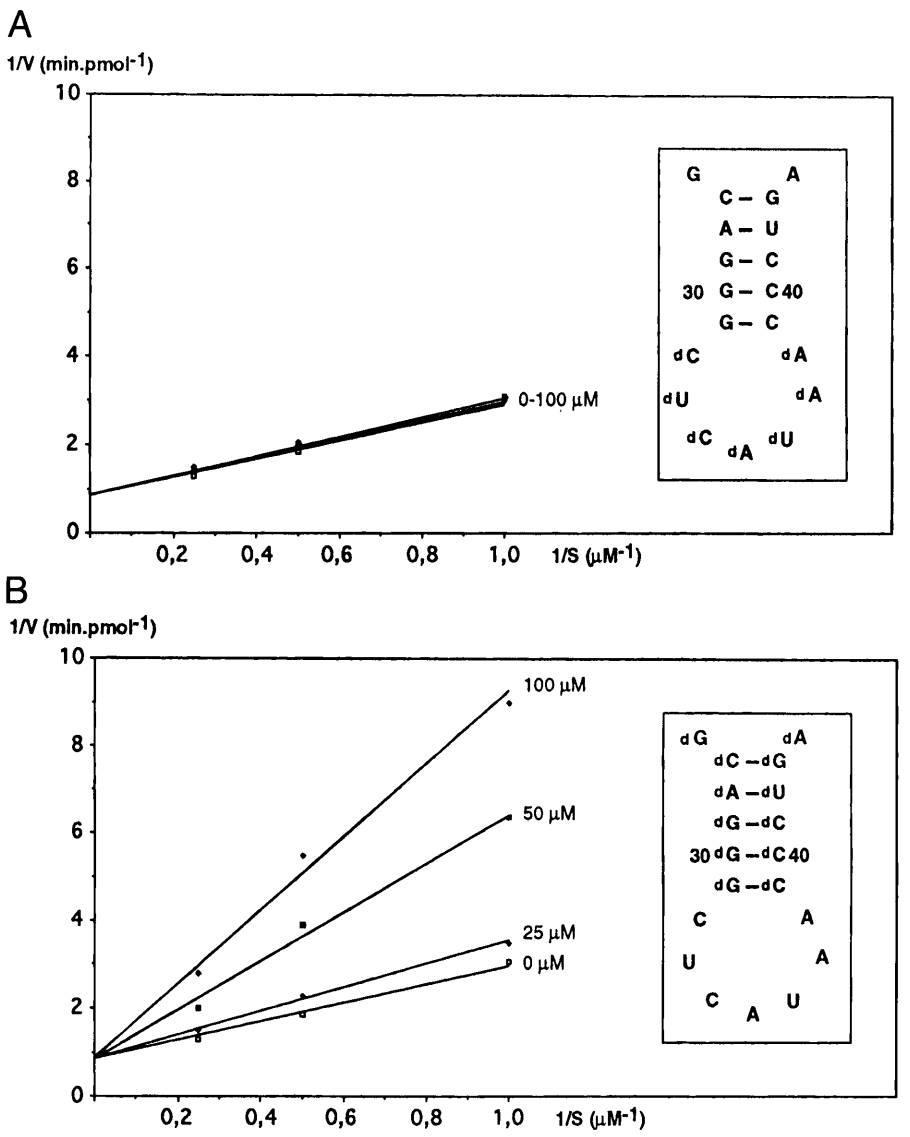

FIGURE 3. Inhibition of yeast $tRNA^{Met}$ aminoacylation by mixed anticodon minihelices. **A:** Aminoacylation in the presence of anticodon minihelix containing a deoxyribose loop. **B:** Aminoacylation in the presence of anticodon minihelix containing a deoxyribose stem. Aminoacylation was performed using 2 μM of yeast $tRNA^{Met}$ and variable minihelix concentrations as indicated in the figure. Kinetics were performed with 5 nM of pure MetRS as described in Materials and Methods.

tively influence the interaction of an anticodon minihelix with the cognate aminoacyl-tRNA synthetase.

TGGE analysis and melting profiles of the $tRNA^{Met}$ U20G60 tertiary mutant involving D-and T-loop interactions

The T- and D-loop of yeast initiator $tRNA^{Met}$ contain a number of sequence features that occur only infrequently in elongator tRNAs (presence of A20 and A54-U55 residues replacing the canonical T-Ψ) and that cluster together in the 3D fold to form a unique substructure at the outer corner of the tRNA (Basavappa & Sigler, 1991). The substructure involving A20 from the D-loop and G57A69A60 from the T-loop is stabilized by an extensive network of hydrogen bonds. The mutation of nt 20 and 60 into U20G60 virtually abolishes $tRNA^{Met}$ aminoacylation (Senger et al., 1995). We show here that the loss of activity does not result from a loss of tRNA binding. Indeed, the tertiary mutant behaves as a competitive inhibitor of wild-type $tRNA^{Met}$ and has a binding constant, deduced from the K_i value of 50 μM (Fig. 4), that is only reduced fivefold from the K_m of $tRNA^{Met}$ (Senger et al., 1995).

To begin identifying the defect responsible for the loss of tRNA function, we used TGGE of radiolabeled wild-type and mutant $tRNA^{Met}$ transcripts. This method, initially introduced to analyze conformational transitions of stable RNAs (viral RNAs and *ompA* mRNA; Riesner et al., 1992) is particularly suited for a study of a tRNA tertiary mutant.

When a gradient of temperature is applied perpendicularly to the direction of migration, nucleic acids in a given conformation migrate as a linear slope in a temperature-dependent manner. Generally, it is be-

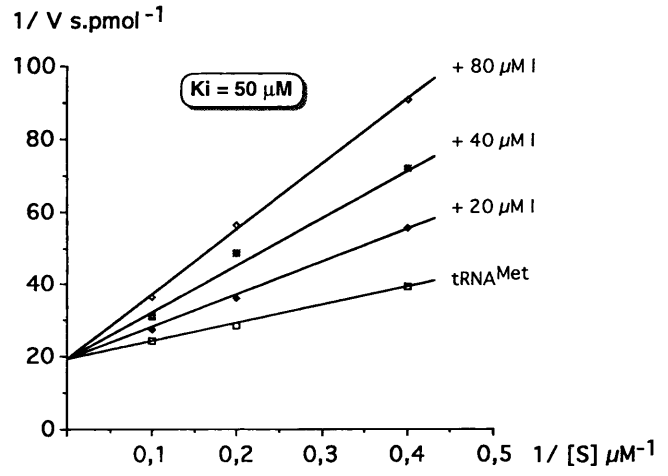

FIGURE 4. Determination of the competitive inhibition constant K_i of $tRNA^{Met}$ U20G60 tertiary mutant. Aminoacylation was measured using of 2.5 μM, 5 μM, and 10 μM native $tRNA^{Met}$ in the presence of the mutant tRNA. The K_i parameter was deduced from plots of $1/V$ versus $1/[S]$. The MetRS concentration used was 5 nM.

lieved that folded nucleic acids migrate faster than denatured forms. Thus, at the point where the structure melts, the slope of migration makes a turn backward because of the lower mobility of the denatured state. TGGE analysis was applied to three different $tRNA^{Met}$ transcripts (Fig. 5): a deoxycytidine analogue of $tRNA^{Met}$ (dC, upper band), wild-type $tRNA^{Met}$ (middle band), and mutant $tRNA^{Met}$ (lower band). The DNA variant of $tRNA^{Met}$ was taken as a control of the tertiary structure melting because this transcript was shown to be less stable than a wild-type transcript (R. Aphasizhev & F. Fasiolo, unpubl. results). The assignment of the different melting curves was deduced from the migration of the individual transcripts on a separate gel (results not shown). Each tRNA shows two clear transitions, numbered 1 and 2. Transition 2 occurs at 65 °C and is common is to all of them; it probably reflects the melting of any $tRNA^{Met}$ secondary structure. Transition 1, which occurs at 32 °C, 43 °C, and 53 °C for dC, wild-type, and mutant $tRNA^{Met}$, respectively, probably reflects the melting of the tertiary structure. Indeed, earlier thermodynamic studies of Crother and coworkers (Cole et al., 1972; Stein & Crothers, 1976) or Coutts et al. (1974) have shown that the first step in the thermal denaturation of a tRNA is composed of the simultaneous melting of the tertiary structure and D-helix, which serves as a nucleus for the tertiary bonds.

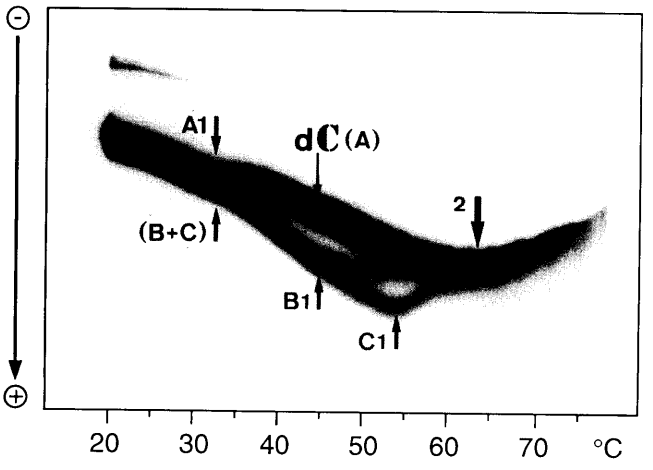

FIGURE 5. TGGE analysis of various $tRNA^{Met}$ transcripts. **A:** Deoxycytidine species of $tRNA^{Met}$. **B,C:** Wild-type and mutant $tRNA^{Met}$, respectively. The first transition for wild-type $tRNA^{Met}$ and $tRNA^{Met}$ U20G60 mutant is indicated by the letters B1 and C1, respectively. Number 2 indicates the melting of the secondary structures for all three tRNA variants.

The difference in thermal stability between the two $tRNA^{Met}$ transcripts is confirmed by the analysis of their melting profiles in the presence or absence of magnesium (Fig. 6). Addition of magnesium to a tRNA is known to preferentially stabilize the native tertiary structure (Stein & Crothers, 1976). In the absence of magnesium, wild-type and mutant $tRNA^{Met}$ structures have T_m values of 57 °C and 65 °C, respectively. The melting profile shows a single thermal transition, indicating that, in solution, the structure of each transcript breaks down cooperatively. When $MgCl_2$ is added to a final concentration of 10 mM, we observe a shift of the T_m to higher temperatures for both tRNAs, indicating that magnesium ions are required to stabilize the tRNA structure. Up to 65 °C, several discrete transitions are observed for the wild-type transcript, whereas, at this temperature, the mutant $tRNA^{Met}$ transcript only begins to melt, full denaturation of the tRNA corresponding to an increase of the hyperchromicity of 0.1 unit of absorbance. Although there is a difference in the experimental values of the last thermal transition seen in the TGGE experiments (obtained at low ionic strength conditions and in the absence of magnesium) and the T_m values measured in solution, both approaches confirm an increase in the stability of the mutant tertiary structure depending on whether $MgCl_2$ is present in the solution.

tRNA structure probing

We probed the structure of the mutant $tRNA^{Met}$ by analyzing RNases T1 and T2 digestion patterns. The results in Figure 7 show the existence of a major structural change in the mutant $tRNA^{Met}$ transcript: G18–G19 nucleotides from the D-loop are no longer accessible to single-stranded T1 RNase. Decreased accessibility to RNase T2 is also observed in the mutant tRNA for D-loop nt 15, 16, and 18. This suggests a more compact structure in the core region of the tRNA involving tertiary nucleotides from the D-loop. The structural difference revealed by the nuclease probes was confirmed by analyzing the lead cleavage pattern. Lead ions cleave specifically and efficiently yeast $tRNA^{Phe}$ between res-

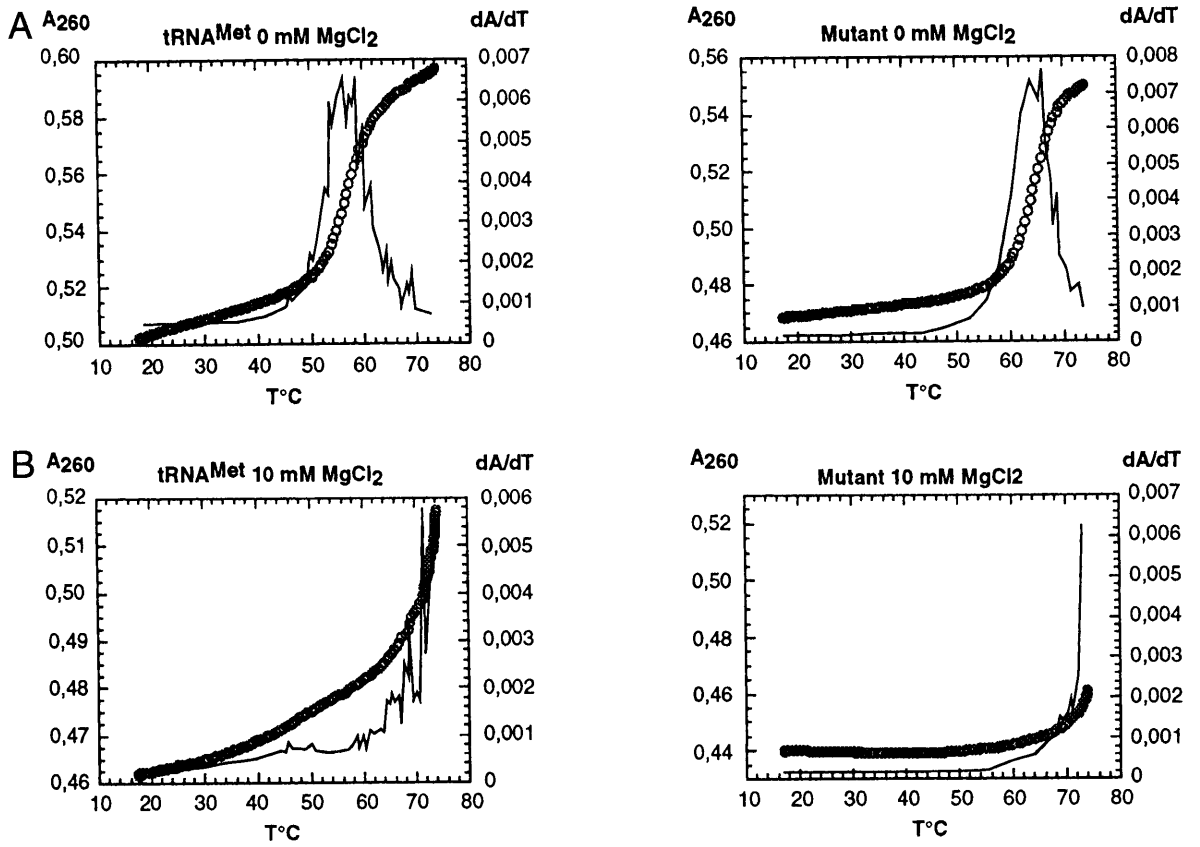

FIGURE 6. Melting curves for wild-type and tRNA^{Met} U20G60 mutant transcripts. Circles show the absorbance at 260 nm. The line indicates the derivative of absorbance versus temperature (dA/dT). **A:** Melting profiles of wild-type and tRNA^{Met} mutant transcripts in the absence of $MgCl_2$. **B:** That obtained in the presence of 10 mM of $MgCl_2$.

idues D17 and G18 because of a very precise geometry of the lead binding pocket (Brown et al., 1985), but more generally, Pb(II) ions have a preferential affinity for interhelical and loop regions (Gornicki et al., 1989). Indeed, major phosphodiester breaks occur in the three loop regions of wild-type tRNA^{Met} transcript, whereas D-loop phosphodiester bonds P19, P20, and P21 from the mutant transcript are no longer susceptible to lead hydrolysis (results not shown). The modification of the nuclease digest or lead hydrolysis pattern suggests a local change in the conformation of the mutant tRNA. An explanation for the increased stability associated with conformational change of the mutant transcript may come from the examination of the yeast initiator tRNA^{Met} crystal structure (Basawappa & Sigler, 1991). In the wild-type, the contacts normally present in elongator tRNAs between G18–G19 and the T-loop are destabilized by the network of tertiary interactions between A20 and G57–A60. The presence of a U instead of an A at position 20 disrupts all those contacts seen in the characteristic initiator substructure between residues 20, 57, and 60. Within this scheme, U20 would be rejected from the D-loop, favoring: (1) the usual contacts of elongator tRNAs between G18–G19 and T-loop residues U55, C56; (2) additional contacts with neighboring nucleotides.

CONCLUSION

In this study, we have analyzed a number of contributions that influence the tRNA^{Met}-MetRS interaction indirectly. We have shown that (1) the integrity of the phosphodiester backbone in the core region responsible for the tertiary fold, or in the functionally strategic anticodon region, is important for tRNA aminoacylation and (2) efficient tRNA^{Met} binding depends on the conformation dictated by a ribosephosphate and not a deoxyribosephosphate backbone. More importantly for the understanding of the role played by the tRNA^{Met} structure in tRNA aminoacylation are the data from the U20G60 tertiary mutant of yeast initiator tRNA^{Met}.

The semiquantitative thermodynamic data (T_m values) and nuclease or chemical probing data of this mutant tRNA^{Met} are consistent and indicate a rearrangement of the tRNA structure that is associated with an increased stability of the tertiary fold. The mutant tRNA^{Met} is still able to bind MetRS with an affinity reduced fivefold compared to that of wild-type tRNA^{Met} transcript, indicating that a severe decrease in the k_{cat} of aminoacylation is responsible for the observed inactivation of the tRNA (Senger et al., 1995). One possible explanation for this k_{cat} defect is that the transition state for aminoacylation requires a particular conformational change, perhaps one that involves flexibility

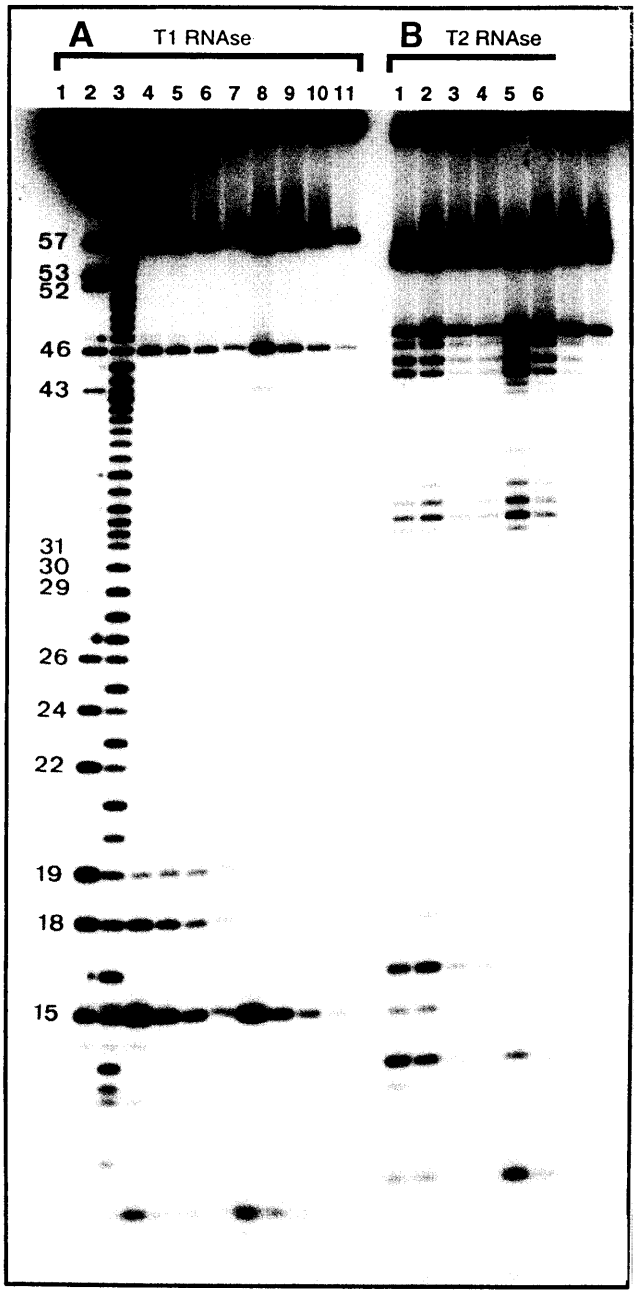

FIGURE 7. Enzymatic probing of the mutant U20G60 $tRNA^{Met}$ transcript. Lanes 1, 2, and 3 correspond to the labeled tRNA, RNAse T1 ladder, and alkali ladder, respectively. **A:** 10 ng, 5 ng, 2 ng, and 1 ng of RNAse A1 are added to wild-type (lanes 4–7) and mutant tRNA (lanes 8–11). **B:** 0.05, 0.05, 0.002, and 0.1 units of RNAse T_2 are added to wild-type (lanes 1–4) and mutant tRNA (lanes 5–8).

of the tRNA structure. In the mutant tRNA, the reduced binding energy available may not be sufficient to overcome the increase of the energetic cost to open the tertiary fold and/or other RNA deformations required for an optimal fit of the acceptor end into the MetRS active site. Loosening or disruption of the D-loop–TΨC-loop interactions upon synthetase binding has been suggested for *E. coli* tRNAs specific for isoleucine (Nureki et al., 1994), methionine (Yamashiro-Matsumura & Kawata, 1981), and valine (Chu & Horowitz, 1991) based on foot-printing and/or NMR experiments.

Functional independence of $tRNA^{Met}$ anticodon binding from acceptor stem interactions with MetRS has been established by dissecting protein–RNA domain–domain interactions in both the tRNA (Meinnel et al., 1991; Gale & Schimmel, 1995; Senger et al., 1995) and the protein (Gale & Schimmel, 1995) and by generating an anticodon-binding deletion mutant having no effect on $tRNA^{Met}$ versus acceptor $microhelix^{Met}$ aminoacylation (Kim & Schimmel, 1992). Recent results with a full-length native MetRS indicate that both the anticodon and the acceptor stem domain contribute significantly to the binding interactions (Gale et al., 1996). Based on the measure of true K_d values, these authors calculated that adding the free energy of binding of the anticodon stem-loop and the $microhelix^{Met}$ provides about 7 kcal/mol of excess binding energy over that needed for intact tRNA. Gale et al. (1996) also found a large difference by about 9 kcal/mol in the apparent free energy of activation for aminoacylation of the microhelix versus $tRNA^{Met}$ based on k_{cat}/K_m values, whereas there is only a minimal difference in the binding energies of the tRNA and minisubstrate. Thus, the excess binding energy generated by linking the anticodon and acceptor stem interactions as occurs in the whole tRNA structure is available for distorting the enzyme–tRNA structure to reach transition state of aminoacylation. With these thermodynamic considerations, the k_{cat} defect of the yeast $tRNA^{Met}$ mutant can be explained by a failure to overcome an increase of the free energetic cost of distorting the more stable tRNA structure. Alternatively, the mutant tRNA could be deficient in inducing a required MetRS conformational change in addition to (or instead of) tRNA-based distorsions.

MATERIALS AND METHODS

Production of $tRNA^{Met}$ fragments

Plasmid pTM1 bearing wild-type $tRNA^{Met}$ gene (Senger et al., 1995) was used to generate $tRNA^{Met}$ fragments 1–28, 29–76, 1–34, 35–76, 1–52, and 9–76 in a two-step procedure: (1) corresponding DNA fragments under the control of the T7 RNA polymerase promoter were produced by PCR; (2) RNA fragments were then synthesized enzymatically using T7 RNA polymerase in the following conditions: 60 mM Tris-HCl, pH 8, 30 mM $MgCl_2$, 7 mM dithiothreitol, 1.4 mM spermidine, 14 mM Triton X-100, 20 mM GMP, 4 mM of each ribonucleotide and T7 RNA polymerase. After 3 h of incubation at 37 °C, the reaction was stopped by addition of 100 μL of 0.5 M EDTA and phenol extraction. The RNA was precipitated by ethanol and resuspended in 250 μL of 50% formamide and purified by PAGE under denaturing conditions. Bands were visualized by UV-shadowing, excised, and electroeluted.

The two short RNA fragments, 1–8 and 53–76, were transcribed directly in the same conditions from a 17-base T7

RNA polymerase promoter top strand annealed to a minus strand oligonucleotide corresponding to the complementary T7 promoter sequence followed by that of the $tRNA^{Met}$ fragment.

Analysis of single-cut $tRNA^{Met}$ variants

To recreate intact $tRNA^{Met}$ molecules, pairs of complementary fragments were mixed together in water to a final concentration of 10–20 μM. Samples are denatured at 100 °C for 1 min, cooled for 20 min at 20 °C before addition of $MgCl_2$ to a final concentration of 10 mM, and the mixture left to stand for 10 min at 20 °C. The resulting hybrids were analyzed at 4 °C on a 10% native polyacrylamide gel using 50 mM Tris-base buffer, pH 8.3, 50 mM boric acid, and 5 mM $MgCl_2$.

Aminoacylation of the hybrids was conducted at 25 °C using 100–500 nM of MetRS in 20 mM HEPES-KOH, pH 7.5, 10 mM $MgCl_2$, 1 mM DTT, 2 mM ATP, 0.1 mM [^{35}S]methionine (1 Ci/mmol, 400–1,500 cpm/pmol).

tRNA structure probing

T1 or T2 ribonuclease digestion of 5′-labeled transcript (100,000 cpm) was performed under native conditions in 10 μL of 20 mM HEPES buffer, pH 7.5, containing 10 mM $MgCl_2$, 50 mM NaCl, and 0.5 μg of carrier $tRNA^{Met}$. After incubation for 5 min at 25 °C, the digestions were stopped by phenol/chloroform extraction and ethanol precipitation. The results were analyzed on a 15% denaturing polyacrylamide gel.

TGGE analysis

Melting of the $tRNA^{Met}$ tertiary mutant was obtained using a TGGE assay (Riesner et al., 1991). Experiments were performed with the DIAGEN-TGGE system (DIAGEN, Hilden, FRG), where a linear temperature gradient was established perpendicularly to the direction of migration. The RNA sample labeled at the 5′ end (10,000 cpm) was loaded into one broad slot of a 12% polyacrylamide gel (acrylamide:bisacrylamide, 29:1) in a 50 mM Tris-base, 50 mM boric acid, and 0.5 mM EDTA buffer, and run for 2 h at 250 V. The RNA was visualized by X-ray autoradiography.

Optical melting curves

Melting curves were measured using a Uvikon 941 Plus spectrophotometer at 260 nm between 15 and 80 °C in a buffer containing 50 mM sodium cacodylate and various concentrations of $MgCl_2$. We used approximately 20 μg of transcript for each curve. The absorbance versus temperature was measured at 0.5 °C intervals. The derivative of the absorbance was calculated from the experimental data obtained.

ACKNOWLEDGMENTS

We thank G. Nussbaum for the skillful technical assistance and A. Hoeft for the oligonucleotide synthesis. We thank E. Westhof for his help in envisioning the structural change in the mutant tRNA and J. Gangloff for helpful discussions. This work was supported by grants form the Centre National de la Recherche Scientifique (CNRS). R.A. was supported by an EMBO short-term fellowship.

Received November 8, 1996; returned for revision December 16, 1996; revised manuscript received February 13, 1997

REFERENCES

Basavappa R, Sigler PB. 1991. The 3 Å crystal structure of yeast initiator tRNA: Functional implications in initiator/elongator discrimination. *EMBO J 10*:3105–3111.

Basti MM, Stuart AT, Lam RG, Agris PF. 1996. Design, biological activity and NMR solution structure of a DNA analogue of yeast $tRNA^{Phe}$ anticodon domain. *Nature Struct Biol 3*:38–44.

Biou V, Yaremchuk A, Tukalo M, Cusack S. 1994. The 2.9 Å crystal structure of *T. thermophilus* seryl-tRNA synthetase complexed with $tRNA^{Ser}$. *Science 263*:1404–1410.

Brown RS, Dewan JC, Klug A. 1985. Crystallographic and biochemical investigation of the lead(II)-catalysed hydrolysis of yeast phenylalanine tRNA. *Biochemistry 24*:4785–4801.

Chu WC, Horowitz J. 1991. Recognition of *Escherichia coli* valine transfer RNA by its cognate synthetase: A fluorine-19 NMR study. *Biochemistry 30*:1655–1663.

Cole P, Yang SK, Crothers DM. 1972. Conformational changes of transfer ribonucleic acid. Equilibrium phase diagram. *Biochemistry 11*:4358–4368.

Coutts S, Gangloff J, Dirheimer G. 1974. Conformational transitions in $tRNA^{Asp}$ (Brewers Yeast). Thermodynamic, kinetic, and enzymatic measurements on oligonucleotide fragments and in the intact molecule. *Biochemistry 13*:3938–3948.

Despons L, Senger B, Fasiolo F, Walter P. 1992. Binding of the yeast $tRNA^{Met}$ anticodon by the cognate methionyl-transfer RNA synthetase involves at least 2 independent peptide regions. *J Mol Biol 225*:897–907.

Draper DE. 1993. Protein–DNA complexes: The cost of recognition. *Proc Natl Acad Sci USA 90*:7429–7430.

Draper DE. 1995. Protein–RNA recognition. *Annu Rev Biochem 64*:593–620.

Gale AJ, Schimmel P. 1995. Isolated RNA binding domain of a class I tRNA synthetase. *Biochemistry 34*:8896–8903.

Gale AJ, Shi JP, Schimmel P. 1996. Evidence that specificity of microhelix charging by a class I tRNA synthetase occurs in the transition state of catalysis. *Biochemistry 35*:608–615.

Giégé R, Puglisi JD, Florentz C. 1993. tRNA structure and aminoacylation efficiency. *Prog Nucleic Acid Res Mol Biol 45*:129–206.

Gornicki P, Baudin F, Romby P, Wiewiorowski M, Kryzosiak W, Ebel JP, Ehresmann C, Ehresmann B. 1989. Use of lead(II) to probe the structure of large RNA's. *J Biomol Struct Dyn 6*:971–1070.

Gott JM, Pan T, LeCuyer KA, Uhlenbeck OC. 1993. Using circular permutation analysis to redefine the R17 coat protein binding. *Biochemistry 32*:13399–13404.

Kim S, Schimmel P. 1992. Functional independence of microhelix aminoacylation from anticodon binding in a class I tRNA synthetase. *J Biol Chem 267*:15563–15567.

Lesser DR, Kurpiewski MR, Jenjacobson L. 1990. The energetic basis of specificity in the Eco RI endonuclease DNA interaction. *Science 250*:776–786.

Lesser DR, Kurpiewski MR, Waters T, Connolly BA, Jen-Jacobson L. 1993. Facilitated distortion of the DNA site enhances *EcoRI* endonuclease–DNA recognition. *Proc Natl Acad Sci USA 90*:7548–7552.

Liu HJ, Musier-Forsyth K. 1994. *Escherichia coli* proline tRNA synthetase is sensitive to changes in the core region of $tRNA^{Pro}$. *Biochemistry 33*:12708–12714.

McClain WH. 1993. Transfer RNA identity. *FASEB J 7*:72–78.

Meinnel T, Mechulam Y, Blanquet S, Fayat G. 1991. Binding of the anticodon domain of $tRNA^{Met}$ to *Escherichia coli* methionyl-tRNA synthetase. *J Mol Biol 220*:205–208.

Musier-Forsyth K, Schimmel P. 1992. Functional contacts of a transfer RNA synthetase with 2′-hydroxyl groups in the RNA minor groove. *Nature 357*:513–515.

Nureki O, Niimi T, Muramatsu T, Kanno H, Kohno T, Florentz C,

Giege R, Yokoyama S. 1994. Molecular recognition of the identity determinant set of isoleucine tRNA from *Escherichia coli*. *J Mol Biol 236*:710–724.

Pan T, Gutell RR, Uhlenbeck OC. 1991. Folding of circularly permuted transfer RNAs. *Science 254*:1361–1364.

Pan T, Uhlenbeck OC. 1993. Circularly permuted DNA, RNA and proteins—A review. *Gene 125*:111–114.

Pan T, Zhong K. 1994. Selection of circularly permuted ribozymes from *Bacillus subtilis* RNAse P by substrate binding. *Biochemistry 33*:14207–14212.

Perona JJ, Rould M, Steitz TA, Risler JL, Zelwer C, Brunie S. 1991. Structural similarities in glutaminyl-transfer RNA and methionyl-transfer RNA synthetases suggest a common overall orientation of transfer RNA binding. *Proc Natl Acad Sci USA 88*:2903–2907.

Riesner D, Henco K, Steger G. 1991. Temperature-gradient gel electrophoresis: A method for the analysis of conformational transitions and mutations in nucleic acids and proteins. In: Chrambach A, Dunn MJ, Radola BJ, eds. *Advances in electrophoresis, 4*. New York: VCH. pp 171–249.

Riesner D, Steger G, Wiese U, Wulfert M, Heibey M, Henco K. 1992. Temperature-gradient gel electrophoresis of polymorphic DNA and for quantitative polymerase chain reaction. *Electrophoresis 13*:632–636.

Rould MA, Perona JJ, Söll D, Steitz TA. 1989. Structure of *E. coli* glutaminyl-tRNA synthetase complexed with tRNA^{Gln} and ATP at 2.8 Å resolution. *Science 246*:1135–1142.

Rould MA, Perona JJ, Steitz TA. 1991. Structural basis of anticodon loop recognition by glutaminyl-transfer RNA synthetase. *Nature 352*:213–218.

Ruff M, Krishnaswamy S, Boeglin M, Poterszman A, Mitschler A, Podjarny A, Rees B, Thierry JC, Moras D. 1991. Class-II aminoacyl tRNA synthetases—Crystal structure of yeast aspartyl-tRNA synthetase complexed with tRNA^{Asp}. *Science 252*:1682–1689.

Saks ME, Sampson JR, Abelson JN. 1994. The tRNA identity problem—A search for rules. *Science 263*:191–197.

Senger B, Aphasizhev R, Walter P, Fasiolo F. 1995. The presence of a D-stem but not of a T-stem is essential for triggering aminoacylation upon anticodon binding in yeast methionine tRNA. *J Mol Biol 249*:45–58.

Senger B, Despons L, Walter P, Fasiolo F. 1992. The anticodon triplet is not sufficient to confer methionine acceptance to a transfer RNA. *Proc Natl Acad Sci USA 89*:10768–10771.

Seong BL, Rajbhandary UL. 1987. *Escherichia coli* formylmethionine tRNA: Mutations in $_{CCC}{}^{GGG}$ sequence conserved in anticodon stem of initiator tRNAs affect initiation of protein synthesis and conformation of anticodon loop. *Proc Natl Acad Sci USA 84*:334–338.

Stein A, Crothers DM. 1976. Equilibrium binding of magnesium(II) by *Escherichia coli* tRNA^{fMet}. *Biochemistry 15*:157–160.

Yamashiro-Matsumura S, Kawata M. 1981. Methionyl-tRNA synthetase-induced conformational change of *Escherichia coli* tRNAf^{Met}. *J Biol Chem 256*:9308–9312.

Yap LI, Musier-Forsyth K. 1995. Transfer RNA aminoacylation: Identification of a critical ribose 2′-hydroxyl-base interaction. *RNA 1*:418–424.

Yarus M, Cline SW, Wier P, Breeden L, Thompson RC. 1986. Actions of the anticodon arm in translation on the phenotypes of tRNA mutants. *J Mol Biol 192*:235–255.